



저작자표시-비영리-변경금지 2.0 대한민국

이용자는 아래의 조건을 따르는 경우에 한하여 자유롭게

- 이 저작물을 복제, 배포, 전송, 전시, 공연 및 방송할 수 있습니다.

다음과 같은 조건을 따라야 합니다:



저작자표시. 귀하는 원저작자를 표시하여야 합니다.



비영리. 귀하는 이 저작물을 영리 목적으로 이용할 수 없습니다.



변경금지. 귀하는 이 저작물을 개작, 변형 또는 가공할 수 없습니다.

- 귀하는, 이 저작물의 재이용이나 배포의 경우, 이 저작물에 적용된 이용허락조건을 명확하게 나타내어야 합니다.
- 저작권자로부터 별도의 허가를 받으면 이러한 조건들은 적용되지 않습니다.

저작권법에 따른 이용자의 권리는 위의 내용에 의하여 영향을 받지 않습니다.

이것은 [이용허락규약\(Legal Code\)](#)을 이해하기 쉽게 요약한 것입니다.

[Disclaimer](#)

의학과 석사 학위논문

**Comparative assessment of virtual monochromatic
reconstruction according to implementation methods
in dual energy computed tomography and its effect on
blooming artifact reduction**

이중 에너지 단층 촬영에서의 구현 방법에 따른
가상 단색 재구성 영상의 비교 평가 및 블루밍 인
공물 감소에 대한 효과 분석

2019년 8월

서울대학교 대학원

의학과 영상의학 전공

한승철

A thesis of the Master's degree

**Comparative assessment of virtual monochromatic
reconstruction according to implementation methods
in dual energy computed tomography and its effect on
blooming artifact reduction**

**이중 에너지 단층 촬영에서의 구현 방법에 따른
가상 단색 재구성 영상의 비교 평가 및 블루밍 인
공물 감소에 대한 효과 분석**

August 2019

Seoul National University College of Medicine

Department of Radiology

Seungchul Han

이중 에너지 단층 촬영에서의 구현 방법에 따른
가상 단색 재구성 영상의 비교 평가 및 블루밍 인
공물 감소에 대한 효과 분석

지도교수 이 활

이 논문을 의학석사 학위논문으로 제출함

2019년 4월

서울대학교 대학원

의학과

한 승 철

한승철의 의학석사 학위논문을 인준함

2019년 7월

위 원 장 구본권 (인)

부위원장 이 활 (인)

위 원 황호영 (인)

Abstract

Comparative assessment of virtual monochromatic reconstruction according to implementation methods in dual energy computed tomography and its effect on blooming artifact reduction

Seungchul Han

Department of Radiology

The Graduate School

Seoul National University

Introduction

Virtual monochromatic images reconstructed by dual energy computed tomography (DECT) are expected to be useful in the discrimination of basic materials and may possibly visualize the K-edge of gadolinium, therefore enhancing material discrimination. Furthermore, virtual monochromatic images reconstructed at high keV levels are believed to reduce

blooming artifact from calcified materials and aid in assessing vascular luminal patency at cardiovascular CT images. However, no previous study compared the three main dual energy implementation methods in discriminating and visualizing the K-edge of basic materials nor provided the objective measurement which proves the superiority of high keV virtual monochromatic images over simply widening the window width in conventional polychromatic images.

Therefore, the purpose of this study is to compare the major three methods of DECT implementation in the perspective of K-edge visualization and material discrimination through spectral attenuation curves in virtual monochromatic reconstruction images. And furthermore, we analyzed high keV monochromatic and conventional polychromatic images to objectively compare the blooming artifacts in a vessel calcification phantom.

Methods

Two different phantoms were scanned by three DECT vendors with different method of dual energy implementation, which are (a) two temporally sequential scans, (b) rapid switching of X-ray tube potential and (c) multilayer detector absorbing photons at different energy level. Spectral attenuation curves of each basic material of Phantom 1 were obtained by monochromatic reconstruction and compared according to vendor and material. Comparison

of blooming artifact between conventional polychromatic and virtual monochromatic images was done by the measurement of Phantom 2 using the full width thirty percent maximum measurement method.

Results

No peak regarding the K-edge of gadolinium was observed in spectral attenuation curves drawn by virtual monochromatic reconstruction of Phantom 1 images regardless of the implementation method or material (calcium, iodine and gadolinium). Material discrimination was possible in all three methods by the slope constant β , and the multilayer detector method showed highest intra-material consistency. In the study with Phantom 2, high kVp polychromatic and high keV monochromatic reconstruction images did not show reduction in measurement error compared to conventional kVp polychromatic images. However, small FOV proved to significantly decrease the blooming artifacts in polychromatic and monochromatic images

Conclusion

Spectral attenuation curves drawn by virtual monochromatic images failed to visualize K-edge regardless of the implementation method or material. High kVp images along with high keV monochromatic reconstruction images failed to reduce blooming artifact, but small FOV proved to significantly

decrease the blooming artifacts in polychromatic and monochromatic images

Keywords

Dual energy computed tomography, Phantom study, Virtual monochromatic reconstruction, K-edge, Blooming artifact

Student Number: 2017-20016

Contents

Abstract in English	1
Contents	5
List of tables and figures	6
Introduction	8
Materials and Methods	11
Results	16
Discussion	24
References	29
Abstract in Korean	33

List of Tables and Figures

Figure 1. Phantom 1 with various concentration of three materials (calcium, iodine, CT materials). Higher concentration at the Left side of the model.

Figure 2. Phantom 2 with 4mm, 3mm, 2mm, 1mm sized hole, compact filling with calcium to measure the blooming artifact.

Figure 3. Attenuation curve of each material (Calcium, Iodine, Gadolinium) drawn by virtual monochromatic reconstruction from three dual energy CT vendors applying different three implementation methods.

Figure 4. Linear conversion of the attenuation curves by logistic conversion and zero adjustment of the intercepts shows linear proximation with slope constant β .

Figure 5. Comparison of slope constant β in three materials (calcium, iodine and gadolinium) according to dual energy implementation method and material concentration.

Figure 6. Figure 6. The mean measurement error of polychromatic images

(above) and monochromatic images (below) according to FOV (218mm, 436mm) and kVp/keV levels. Specific p-values regarding comparison between different FOV is annotated at each kVp/keV level.

Figure 7. Comparison of mean measurement error between monochromatic images and conventional polychromatic images at low kVp (above) and high kVp (below) at 218mm FOV. Specific p-values regarding each keV level is annotated.

Introduction

Dual energy computed tomography (DECT) is now a well-known and widely applicable technique among researchers and practitioners in the field of computed tomography (CT) (1, 2). In contrast to conventional CT, it takes advantage in decomposing the tissue into its components through dual emission or absorption of photons at different energy levels (3-5).

Currently, there are various available methods for the implementation of dual energy among manufacturers. The major three methods available are (a) two temporally sequential scans, (b) rapid switching of X-ray tube potential and (c) multilayer detector absorbing photons at different energy level. There are previous studies comparing these methods and some of those showed inter-manufactural variability in accuracy of iodine quantification (3, 6).

Virtual monochromatic reconstruction is one of the implementations of DECT to synthesize a monochromatic image with obtained polychromatic images (7-9). In contrast to a polychromatic beam which consists of a wide spectrum of photon energy, a monochromatic beam theoretically may show a jump in photoelectric absorption at the binding energy of a K shell electron in a specified material, which we call the 'K-edge'. As K-edge appears at different energy level in different materials, visualizing the K-edge may aid in

further discriminating materials (10). And it is also well known that spectral attenuation curves based on monochromatic reconstruction is one of the qualitative methods in discrimination of different materials (11, 12). However, there is no previous study comparing the three dual energy implementation methods in the ability to clarify the K-edge of basic materials (iodine, gadolinium, calcium) and discriminate these materials through spectral curves obtained by virtual monochromatic reconstruction.

Another believed advantages of monochromatic image compared to conventional polychromatic image is the reduction of blooming artifact in high keV reconstruction images. Blooming artifact is a major issue in cardiovascular imaging which causes the overestimation of calcium plaques leading to underestimation of vascular lumen. It is explained as a result of partial volume artifact, beam hardening artifact and some motion artifact (13, 14). Several approaches were done in previous studies to reduce the blooming artifact including the usage of high kVp imaging, which was previously believed to reduce the partial volume and beam hardening artifact (13). However, as the acquisition of high kVp polychromatic images is practically limited due to technical matter and also due to the radiation dose issue, monochromatic image reconstructed in high keV level has become a promising method that may theoretically reduce the blooming artifact induced by vessel calcification in vascular imaging (7, 15, 16).

However, to our recent knowledge there is a lack of study which provides the objective measurement proving the superiority of high keV virtual monochromatic images over simply widening the window width. As the overall attenuation decreases in high keV images, this may show similar effect with widening the window width and therefore the reduction of blooming artifact may be subjectively overestimated.

Therefore, the purpose of this study is to compare the major three methods of DECT implementation in the perspective of K-edge visualization and material discrimination through spectral attenuation curves in virtual monochromatic reconstruction images. And furthermore, we analyzed monochromatic and conventional images to objectively compare the blooming artifacts in a vessel calcification phantom.

Materials and Methods

This study is a phantom study including three vendors from different manufacturers (Philips, Seimens, GE). Each vendor used a different method for implementation of dual energy source as followed. (a) Philips IQon CT, dual layer detector, (b) Siemens Force, temporally sequential scans via dual beam source and (c) GE HD750, rapid switching of X-ray tube potential. Two phantoms were created and was scanned in each vendor. Approval by the institutional review board was waived.

Phantom design

Two phantoms were designed for different purposes. Phantom 1 was to compare the virtual monochromatic images in the perspective of K-edge visualization and material discrimination in each vendor. Mixture of iodine, gadolinium and calcium in distilled water was made in different concentrations (ioxithalamate 1:16, 1:32, 1:64, 1:128, 1:256; Gadoterate meglumine 1:4, 1:8, 1:16, 1:32, 1:64; Calcium hydroxyapatite 200mg/ml, 150mg/ml, 100mg/ml, 50mg/ml, 25mg/ml) and was contained in a 15cc plastic conical tube (Fig. 1). The concentration of the solutions was aimed for the physiologic level of intravascular HU in practical CT scans.

And for the measurement of blooming artifact, Phantom 2 was designed by creating 4mm, 3mm, 2mm, and 1mm sized pits in polyacrylic base and was compactly filled with calcium hydroxyapatite powder and droplets of distilled water. A total of 16 pits with 4 pits for each size was created (Fig. 2).

CT protocols and reconstruction

All CT scans were performed in helical scan. For phantom 1, the radiation dose was adjusted at CTDI_{vol} of 10.8mGy for each scan, which is a conventional CT dose in noncontrast abdominal CT in our institute. The peak kilovoltage in Philips IQon and GE HD750 was 120kVp, and in Siemens FORCE vendor dual source of 80-140kVp was used. FOV was fixed at 170x170mm for Phantom 1. For phantom 2, conventional polychromatic scans were done at 80, 100, 120, 140 kVp in different FOV (large FOV: 436mm, small FOV: 218mm) for control. Dual energy scan was done in each vendor with the same protocol as phantom 1 except for the adjustment of effective mAs at 150mAs.

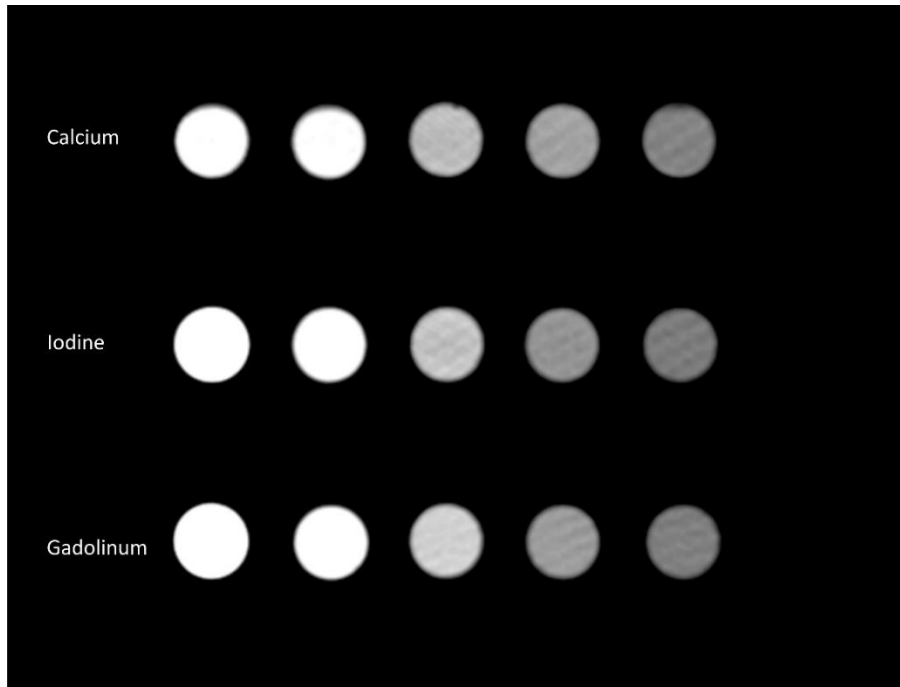


Figure 1. Phantom 1 with various concentration of three materials (calcium, iodine, CT materials). Higher concentration at the Left side of the model.

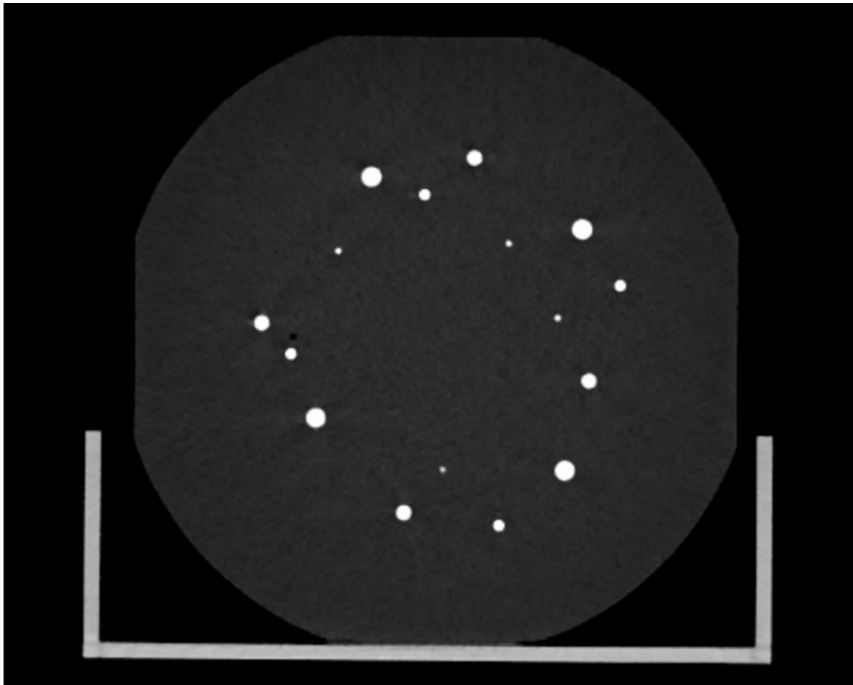


Figure 2. Phantom 2 with 4mm, 3mm, 2mm, 1mm sized hole, compact filling with calcium to measure the blooming artifact.

Virtual monochromatic reconstruction was done through each proved software (Siemens Force; Syngo.via, GE HD750; A/W server 2, Philips IQon CT; Philips ISP). Reconstruction was done from available 40-190keV by 1keV interval at 40-60 keV section to visualize k-edge of iodine and gadolinium, and by 5 keV interval in other sections. Measurement of mean Hounsfield unit in Phantom 1 was done by drawing at ROI larger than 1cm^2 at the center of the phantom. Measurement of blooming artifact in Phantom 2 was done by comparing 80, 100, 120, 140kVp polychromatic source image and

monochromatic reconstruction image at 40, 70, 100, 130, 160, 190keV. After measuring the attenuation of the polyacrylic base and the peak center attenuation of each calcium pit, the largest diameter of each calcium pit was measured at the window level of full width at thirty percent maximum method.

Statistical analysis

In Phantom 1, Hounsfield units for each material and concentration at different keV levels was plotted to form a spectral attenuation curve to visualize the K-edge. Measurements in Phantom 2 was presented in mean value. Wilcoxon signed-rank test and Friedman test was used to compare paired continuous variables. All statistical analyses were performed using SPSS software (version 22; SPSS Inc., Chicago, Illinois), and $p < 0.05$ was considered statistically significant.

Results

Spectral attenuation curves

All three methods showed a similar negative relationship of attenuation with the increment of keV, but none of them were able to visualize the K edge itself or demonstrate a change in slope at the similar energy level in each material (calcium, iodine and gadolinium) (Fig. 3). The trendline of each curve showed a negative exponential function as below with constant β referring to the slope of each curve.

$$HU = \alpha x^{-\beta}$$

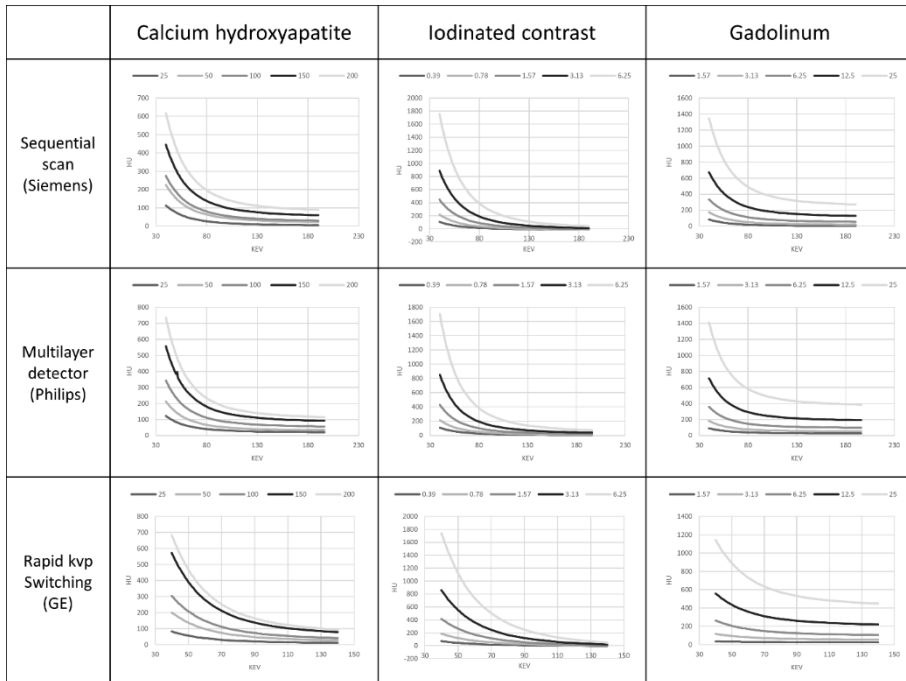


Figure 3. Attenuation curve of each material (Calcium, Iodine, Gadolinium) drawn by virtual monochromatic reconstruction from three dual energy CT vendors applying different three implementation methods.

In order to compare of the constant β in each material, natural logistic conversion was done in each side of the function. The intercept was adjusted to zero and the slope was converted to positive value for intuitive comprehension (Fig. 4).

$$-\ln(HU) = -\ln \alpha + \beta \ln x$$

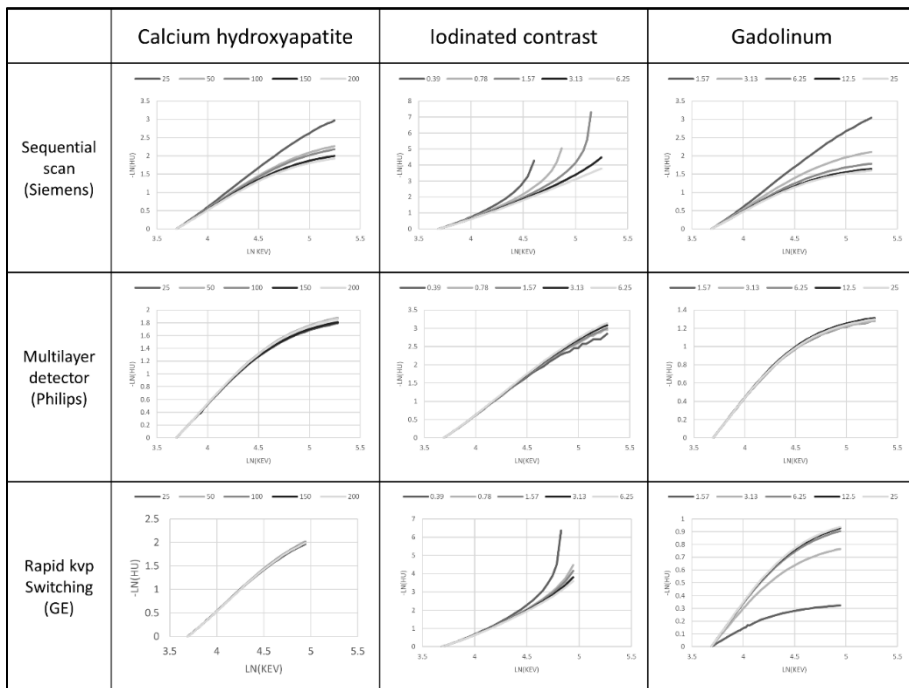


Figure 4. Linear conversion of the attenuation curves by logistic conversion

and zero adjustment of the intercepts shows linear proximation with slope constant β .

In contrast to the multilayered detector method which showed similar β value in the same material despite different concentration, other methods showed different β value of the slope in different concentration especially in high keV reconstructions. Only calcium in rapid kVp switching method showed consistent β value. In case of low concentration of iodine, the rapid switching method and the sequential scan method showed a rapid increment of the slope in higher photon energy levels (Fig. 4).

When comparing the three materials in similar attenuation levels at conventional 120kVp image, all three materials were all separated in rapid kVp switching and multilayer detector method, but calcium and gadolinium showed similar slope constant in sequential scan method. (Fig. 5)

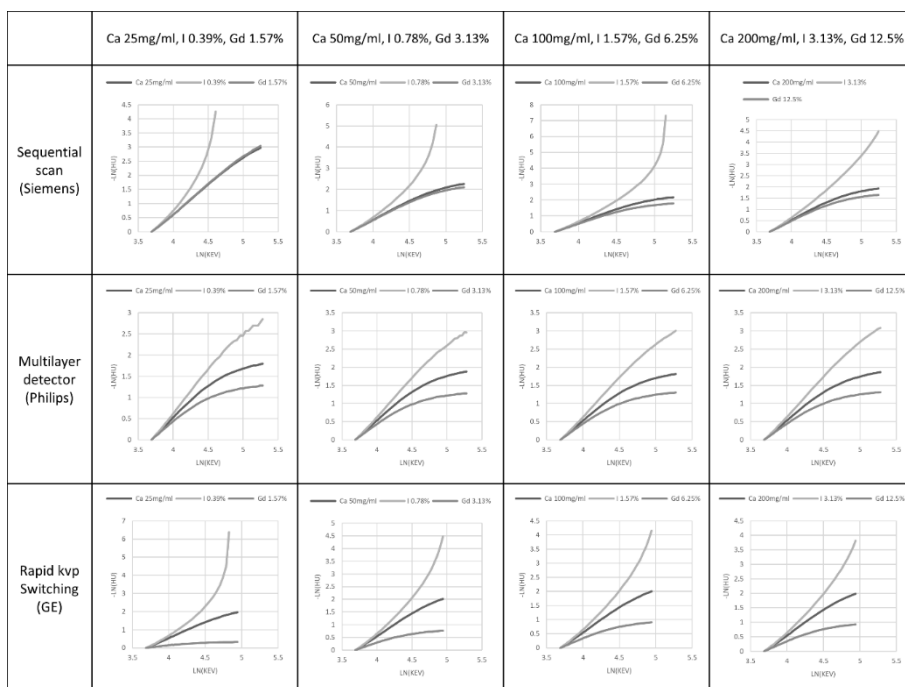
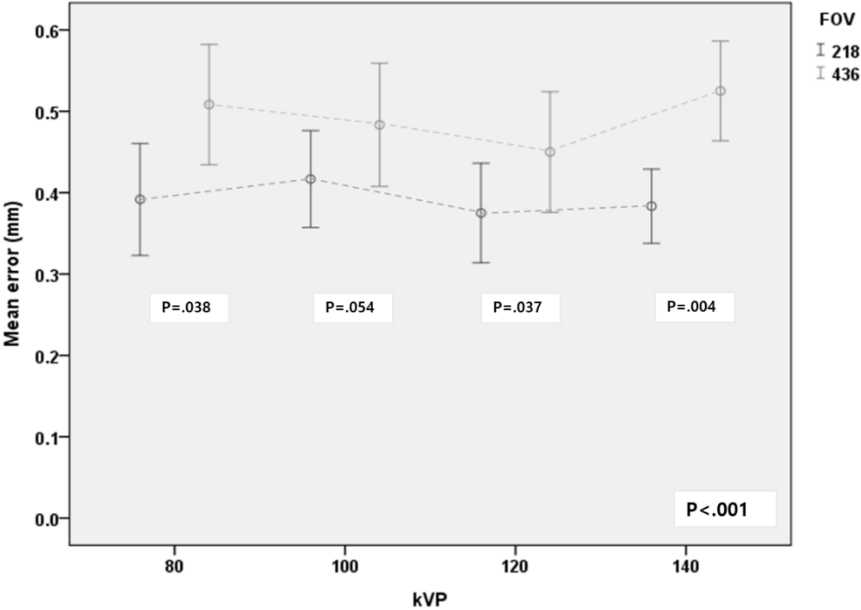


Figure 5. Comparison of slope constant β in three materials (calcium, iodine and gadolinium) according to dual energy implementation method and material concentration.

Blooming artifact

The mean error in measurement due to blooming artifact was largest in 40keV monochromatic reconstruction image with large FOV (mean value $0.70 \pm 0.15\text{mm}$) and smallest in 120kVp polychromatic image with small FOV (mean value $0.38 \pm 0.10\text{mm}$). Small FOV images showed significantly small measurement error compared to large FOV images in both polychromatic and monochromatic images ($P < 0.001$). However, there was no significant

difference in polychromatic images according to kVp levels in both large and small FOV images (218mm, P=0.34 and 436mm, P=0.12). Also, there was no significant difference in monochromatic reconstruction images according to reconstructed keV levels in both FOV images (218mm, P=0.72 and 436mm, P=0.57) (Fig. 6). The mean value of measurement error was significantly larger in monochromatic reconstruction images compared to polychromatic images especially in low keV levels (Fig. 7).



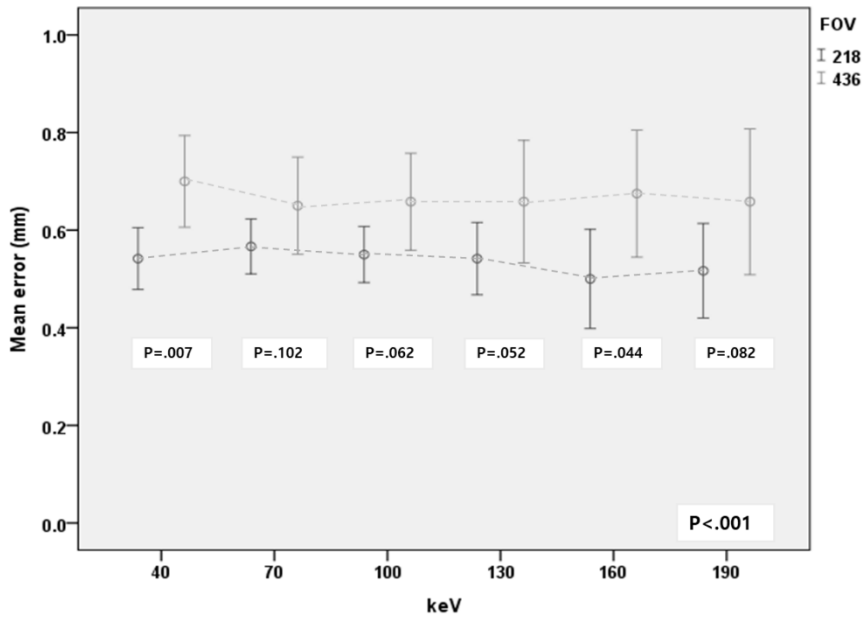


Figure 6. The mean measurement error of polychromatic images (above) and monochromatic images (below) according to FOV (218mm, 436mm) and kVp/keV levels. Specific p-values regarding comparison between different FOV is annotated at each kVp/keV level.

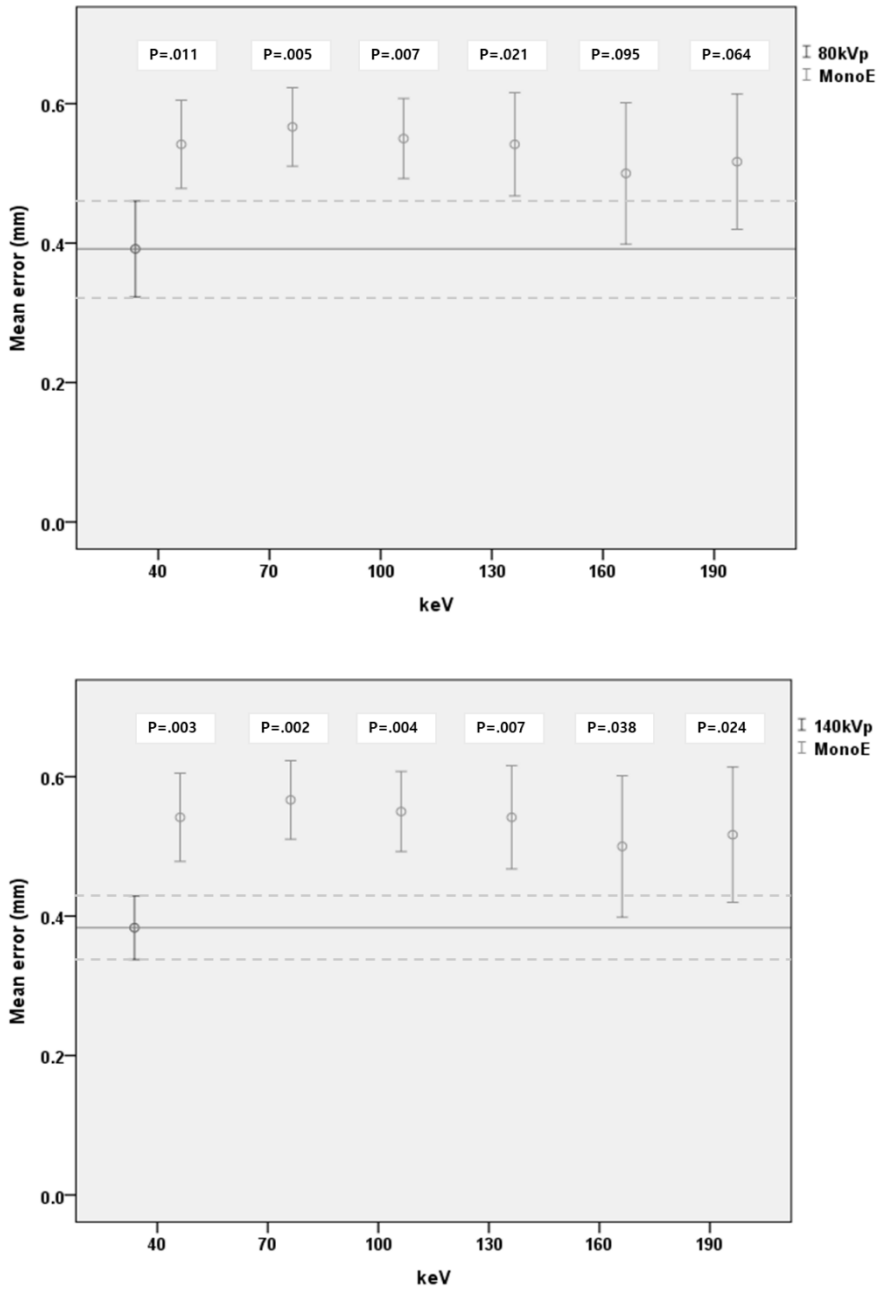


Figure 7. Comparison of mean measurement error between monochromatic images and conventional polychromatic images at low kVp (above) and high

kVp (below) at 218mm FOV. Specific p-values regarding each keV level is annotated.

Discussion

In the current study, all three vendors with different dual energy implementation failed to visualize the K-edge of materials in monochromatic reconstruction images. As the synthesis of virtual monochromatic imaging is an indirect modeling with the assumption of multiple basis materials based on either projection or image domain, resolution along the photon energy domain might not be precise enough to visualize the ‘peak’ at the level of K shell binding energy. This could be overcome in a more precise and direct technology including the introduction of photon counting detector (9, 10, 12). Currently there are several studies of K-edge imaging using the photon counting detector but has not been yet commercialized. One of the main technical issue is the count rate limitation of the detectors which cannot cope with the photon fluxes in conventional CT scans (10, 17). Once K-edge imaging becomes available in practice, not only the discrimination of contrast materials but discrimination of other specific materials according to atomic number may become theoretically possible.

All three vendors in the study showed different slope values (which was referred as constant β in this study) of spectral attenuation curve according to materials, which can be the basis of material differentiation (3, 9, 12, 18).

However, the sequential scanning method showed relatively poor differentiation of calcium and gadolinium compared to other methods. And in the aspect of reproducibility of the constant β , multilayer detector method showed the highest consistency according to the material despite different concentrations. Other methods generally showed lower slope values with increasing concentrations, except for gadolinium in rapid kVp switching method, which showed the opposite trend. Although this cannot be clearly understood, the difference might be due to the different algorithm among vendors and the different domain in which the process is done (4).

Analysis of Phantom 2 CT scans failed to show reduction of blooming artifact in high keV or kVp images. Instead, virtual monochromatic images rather showed larger measurement error compared to polychromatic image in contrast to previous belief (2, 9, 16). Previous belief that high kVp image may reduce blooming artifact is based on several researches including phantom and clinical studies showing the reduction of metal artifact in virtual monochromatic images (2, 9, 12). These studies were generally aimed to reduce metal artifacts which is exclusively due to beam hardening artifact and it is widely acknowledged that beam hardening is reduced in high kVp images and theoretically eliminated in virtual monochromatic images (15, 19). Although a portion of blooming artifact is thought to be beam hardening, the results of our study suggest that beam hardening effect reduction by

monochromatic reconstruction is insufficient to eliminate blooming artifact. Other components including partial volume artifact may play a crucial role.

As the blooming artifact owes a major portion to the partial volume artifact, widening the image window is routinely used among radiologists for the reduction of blooming in conventional polychromatic images. Therefore, evaluating the effect in blooming artifact reduction in terms of other technical methods should be done with excluding the effect from widening the image window. There are also few studies that propose the reduction of blooming artifact in coronary stents, but the results of these studies are mostly semi-quantitative and lacks objective measurement (13, 20). One of the adjustment methods for objective measurement which was used in previous studies was to fix the window level and width of the image during the measurement of artifact. However irrespective of the fixed window, high kVp and high keV imaging results in overall decreased attenuation of stent, calcification and surrounding tissue which shows an additional effect of widening the window width. Therefore, in this case, the reduction of blooming artifact cannot be explained independently from the effect of window widening. In the current study, measurement was done by the full width at thirty percent maximum method which absolutely excludes the effect of window width. The results of our study suggest that the objective measurement based on full width at thirty percent maximum method does not reveal the reduction of blooming artifact

in calcified materials. Furthermore the improvement of measurement error in small FOV images might infer that blooming artifact in small vessel with calcification is greatly influenced by limited spatial resolution and the partial volume averaging of different densities (21). Monochromatic reconstruction can theoretically eliminate the beam hardening effect but cannot solve the spatial resolution issue.

This study has several limitations. First, the analysis of spectral attenuation curves was done by a semiquantitative method based on serial virtual monochromatic images. The logistic conversion and the use of constant β for evaluating the slope may be somewhat artificial and intentional. For further quantitative analysis, the use of Z-effective calculation can be considered which provides information on calculated atomic numbers. This algorithm is also available in the three vendors and needs comparative evaluation. Second, only limited number of three major vendors available in our institute were enrolled in the study despite of other various vendors in each implementation methods. There are latest vendors available which composes an up-to-date algorithm compared to our vendors. Further studies in such vendors are necessary due to their various applications (6). Third, analysis of interobserver correlation in the measurement of Phantom 2 calcium pits were not included in the study. Although the full width at maximum method is a well-known objective measurement method, there can be intra- and inter-

observer variability in determining the peak center attenuation and there can be measurement difference in the longest diameter. Repetitive measurement with multiple readers is required to assess the reproducibility of the results of our study. Finally, the study did not contain one of the most important issues in cardiovascular imaging, which are coronary stents. As coronary stents are composed of metallic substance, they might show different features from calcified materials in reconstruction images. However, the measurement of the artifact in coronary stents may not be as straight forward as calcium pits, as it is a circumferential structure with an internal lumen. Further investigation is needed for the evaluation of coronary stent imaging in DECT.

In conclusion, spectral attenuation curves drawn by virtual monochromatic images failed to visualize K-edge regardless of the implementation method or material. High kVp images along with high keV monochromatic reconstruction images failed to reduce blooming artifact, but small FOV proved to significantly decrease the blooming artifacts in polychromatic and monochromatic images.

References

1. Coursey CA, Nelson RC, Boll DT, Paulson EK, Ho LM, Neville AM, et al. Dual-energy multidetector CT: how does it work, what can it tell us, and when can we use it in abdominopelvic imaging? *Radiographics* : a review publication of the Radiological Society of North America, Inc. 2010;30(4):1037-55.
2. Machida H, Tanaka I, Fukui R, Shen Y, Ishikawa T, Tate E, et al. Dual-Energy Spectral CT: Various Clinical Vascular Applications. *Radiographics* : a review publication of the Radiological Society of North America, Inc. 2016;36(4):1215-32.
3. Gabbai M, Leichter I, Mahgerefteh S, Sosna J. Spectral material characterization with dual-energy CT: comparison of commercial and investigative technologies in phantoms. *Acta radiologica* (Stockholm, Sweden : 1987). 2015;56(8):960-9.
4. McCollough CH, Leng S, Yu L, Fletcher JG. Dual- and Multi-Energy CT: Principles, Technical Approaches, and Clinical Applications. *Radiology*. 2015;276(3):637-53.
5. Johnson TR. Dual-energy CT: general principles. *AJR American journal of roentgenology*. 2012;199(5 Suppl):S3-8.

6. Jacobsen MC, Schellingerhout D, Wood CA, Tamm EP, Godoy MC, Sun J, et al. Intermanufacturer Comparison of Dual-Energy CT Iodine Quantification and Monochromatic Attenuation: A Phantom Study. *Radiology*. 2018;287(1):224-34.
7. Danad I, Fayad ZA, Willeminck MJ, Min JK. New Applications of Cardiac Computed Tomography: Dual-Energy, Spectral, and Molecular CT Imaging. *JACC Cardiovascular imaging*. 2015;8(6):710-23.
8. Goodsitt MM, Christodoulou EG, Larson SC. Accuracies of the synthesized monochromatic CT numbers and effective atomic numbers obtained with a rapid kVp switching dual energy CT scanner. *Medical physics*. 2011;38(4):2222-32.
9. Yu L, Leng S, McCollough CH. Dual-energy CT-based monochromatic imaging. *AJR American journal of roentgenology*. 2012;199(5 Suppl):S9-s15.
10. Meng B, Cong W, Xi Y, De Man B, Yang J, Wang G. Model and reconstruction of a K-edge contrast agent distribution with an X-ray photon-counting detector. *Optics express*. 2017;25(8):9378-92.
11. Johnson TR, Krauss B, Sedlmair M, Grasruck M, Bruder H, Morhard D, et al. Material differentiation by dual energy CT: initial experience. *European radiology*. 2007;17(6):1510-7.
12. Patino M, Prochowski A, Agrawal MD, Simeone FJ, Gupta R, Hahn

PF, et al. Material Separation Using Dual-Energy CT: Current and Emerging Applications. *Radiographics* : a review publication of the Radiological Society of North America, Inc. 2016;36(4):1087-105.

13. Kalisz K, Buethe J, Saboo SS, Abbara S, Halliburton S, Rajiah P. Artifacts at Cardiac CT: Physics and Solutions. *Radiographics* : a review publication of the Radiological Society of North America, Inc. 2016;36(7):2064-83.

14. Li P, Xu L, Yang L, Wang R, Hsieh J, Sun Z, et al. Blooming Artifact Reduction in Coronary Artery Calcification by A New De-blooming Algorithm: Initial Study. *Sci Rep*. 2018;8(1):6945.

15. Bamberg F, Dierks A, Nikolaou K, Reiser MF, Becker CR, Johnson TR. Metal artifact reduction by dual energy computed tomography using monoenergetic extrapolation. *European radiology*. 2011;21(7):1424-9.

16. Yu L, Christner JA, Leng S, Wang J, Fletcher JG, McCollough CH. Virtual monochromatic imaging in dual-source dual-energy CT: radiation dose and image quality. *Medical physics*. 2011;38(12):6371-9.

17. Roessl E, Proksa R. K-edge imaging in x-ray computed tomography using multi-bin photon counting detectors. *Physics in medicine and biology*. 2007;52(15):4679-96.

18. Forghani R, Levental M, Gupta R, Lam S, Dadfar N, Curtin HD. Different spectral hounsfield unit curve and high-energy virtual

monochromatic image characteristics of squamous cell carcinoma compared with nonossified thyroid cartilage. *AJNR American journal of neuroradiology*. 2015;36(6):1194-200.

19. Codari M, de Faria Vasconcelos K, Ferreira Pinheiro Nicolielo L, Haiter Neto F, Jacobs R. Quantitative evaluation of metal artifacts using different CBCT devices, high-density materials and field of views. *Clinical oral implants research*. 2017;28(12):1509-14.

20. Suzuki S, Furui S, Kuwahara S, Kaminaga T, Yamauchi T, Kawasaki T, et al. Assessment of coronary stent in vitro on multislice computed tomography angiography: improved in-stent visibility by the use of 140-kV tube voltage. *Journal of computer assisted tomography*. 2007;31(3):414-21.

21. Li P, Xu L, Yang L, Wang R, Hsieh J, Sun Z, et al. Blooming Artifact Reduction in Coronary Artery Calcification by A New De-blooming Algorithm: Initial Study. *Scientific Reports*. 2018;8(1):6945.

요약 (국문초록)

서론

이중 에너지 컴퓨터 단층 촬영 (DECT)에서 구현하는 가상 재구성 단색영상의 경우 바탕 물질을 구분하고 더 나아가 물질의 K-edge를 시 각화함으로써 물질 차별화에 도움을 줄 수 있을 것으로 기대되는 기술이다. 또한 높은 keV 수준으로 재구성된 가상 단색영상의 경우 석회화된 물질에서 발생하는 블루밍 인공물을 감소시킴으로서 심혈관 영상에서 혈관 내경을 평가하는 데에 도움을 줄 수 있는 것으로 믿어지고 있다. 하지만 현재까지는 주요 3가지 이중 에너지 구현방식에 따라서 물질의 구분하고 K-edge를 구현할 수 있는지 여부를 연구한 논문은 없으며, 또한 정확한 측정을 통해 높은 keV의 가상 단색구성 영상이 통상적인 다색구성 영상의 window를 단순히 넓히는 것보다 블루밍 인공물을 감소시킨다는 것을 밝힌 연구 또한 없다. 따라서 본 연구의 목적은 가상 단색구성 영상을 통해 얻은 스펙트럴 곡선으로 DECT의 주요 3가

지 구현방식에 따라서 K-edge를 시각화하고 물질을 구분할 수 있는지를 우선 평가하고, 더 나아가 혈관 석회화 팬텀을 통하여 높은 keV 가 상 단색 재구성 영상에서 블루밍 인공물 감소여부를 평가한다.

방법

서로 다른 2개의 팬텀을 제작하여 이중 에너지의 구현 방식이 다른 세 종류의 DECT 기기를 통해 촬영한다. 이 세가지 구현방식은 (a) 2개의 튜브를 통한 순차 스캔, (b) 빠른 X 선관 전위 스위칭, 그리고 (c) 상이한 에너지 레벨의 광자를 흡수하는 다층 검출기의 사용과 같다. 이러한 팬텀 1 스캔 영상을 가상 단색영상으로 재구성하여 물질에 따른 스펙트럼 감쇠 곡선을 구성하였다. 그리고 팬텀 2 스캔 영상을 사용한 full width thirty percent maximum 방법의 측정을 통하여 블루밍 인공물로 인해 발생하는 오차를 가상 단색영상과 통상적인 다색영상에서 비교하였다.

결과

팬텀 1 촬영 영상의 가상 단색 재구성에 의해 얻어진 스펙트럼 감소 곡선은 구현 방법이나 재료 (칼슘, 요오드 및 가돌리늄)에 관계없이 K-edge를 시각화하지 못하였다. 그러나 감소곡선의 기울기 상수 β 를 활용한 물질의 식별은 3 가지 방법 모두에서 가능하였고, 기울기 상수 β 값은 다층 검출기 방법에서 재료 내 일관성이 가장 뚜렷하였다. 또한 팬텀 2 촬영영상에서 높은 kVp 영상과 높은 keV 가상 단색 구성영상은 측정오류를 감소시키지 못하였으나 작은 FOV의 다색 및 가상 단색 재구성 영상은 큰 FOV 영상보다 통계적으로 유의하게 블루밍 인공물을 감소시켰다 ($P < 0.05$).

결론

가상 단색영상 재구적으로 그린 스펙트럼 감소 곡선은 구현 방법이나 재료에 관계없이 K 에지를 시각화하지 못하였다. 높은 kVp 영상과 높은 keV 가상 단색 구성영상은 블루밍 인공물을 감소시키는 데에 실패하였으나 작은 FOV를 갖는 영상의 경우 기존 영상에 비해 블루밍

인공물을 유의하게 감소시키는 것으로 나타났다

주요어 : 이중 에너지 컴퓨터 단층 촬영, 팬텀 연구, 가상 단색영상 재구

성, K-edge, 블루밍 인공물

학 번 : 2017-20016